Isospin Character of Low-Lying Pygmy Dipole States in ^{208}Pb via Inelastic Scattering of ^{17}O Ions

F. C. L. Crespi,[1,2] A. Bracco,[1,2,*] R. Nicolini,[1,2] D. Mengoni,[3,4] L. Pellegri,[1,2] E. G. Lanza,[5] S. Leoni,[1,2] A. Maj,[6] M. Kmiecik,[6] R. Avigo,[1,2] G. Benzoni,[2] N. Blasi,[2] C. Boiano,[2] S. Bottoni,[1,2] S. Brambilla,[2] F. Camera,[1,2] S. Ceruti,[1,2] A. Giaz,[2] B. Million,[2] A. I. Morales,[1,2] V. Vandone,[1,2] O. Wieland,[2] P. Bednarczyk,[6] M. Ciemała,[6] J. Grebosz,[6] M. Krzysiek,[6] K. Mazurek,[6] M. Zieblinski,[6] D. Bazzacco,[4] M. Bellato,[4] B. Birkenbach,[7] D. Bortolato,[3,4] E. Calore,[8] B. Cederwall,[9] L. Charles,[10] G. de Angelis,[8] P. Désesquelles,[11] J. Eberth,[7] E. Farnea,[4] A. Gadea,[12] A. Görgen,[13] A. Gottardo,[3,8] R. Isocrate,[4] J. Jolie,[7] A. Jungclaus,[14] N. Karkour,[11] W. Korten,[15] R. Menegazzo,[4] C. Michelagnoli,[3,4] P. Molini,[8] D. R. Napoli,[8] A. Pullia,[1,2] F. Recchia,[3,4] P. Reiter,[7] D. Rosso,[8] E. Sahin,[8,†] M. D. Salsac,[15] B. Siebeck,[7] S. Siem,[13] J. Simpson,[16] P.-A. Söderström,[17,‡] O. Stezowski,[18] Ch. Theisen,[15] C. Ur,[4] and J. J. Valiente-Dobón[8]

[1]*Dipartimento di Fisica dell'Università degli Studi di Milano, I-20133 Milano, Italy*
[2]*INFN, Sezione di Milano, I-20133 Milano, Italy*
[3]*Dipartimento di Fisica dell'Università degli Studi di Padova, I-35131 Padova, Italy*
[4]*INFN, Sezione di Padova, I-35131 Padova, Italy*
[5]*INFN, Sezione di Catania, I-95123 Catania, Italy*
[6]*The Niewodniczanski Institute of Nuclear Physics, PAN, 31-342 Krakow, Poland*
[7]*Institut für Kernphysik, Universität zu Köln, D-50937 Köln, Germany*
[8]*INFN, Laboratori Nazionali di Legnaro, Legnaro I-35020, Italy*
[9]*Department of Physics, Royal Institute of Technology, SE-10691 Stockholm, Sweden*
[10]*Institut Pluridisciplinaire Hubert Curien IPHC, CNRS/IN2P3 and Université de Strasbourg BP 28, F-67037 Strasbourg Cedex 2, France*
[11]*Centre de Spectrométrie Nucléaire et de Spectrométrie de Masse CSNSM, CNRS/IN2P3 and Université Paris-Sud, F-91405 Orsay Campus, France*
[12]*IFIC, CSIC-Universitat de València, E-46980 València, Spain*
[13]*Department of Physics, University of Oslo, N-0316 Oslo, Norway*
[14]*Instituto de Estructura de la Materia, CSIC, Madrid, E-28006 Madrid, Spain*
[15]*Institut de Recherche sur les lois Fondamentales de l'Univers IRFU, CEA/DSM, Centre CEA de Saclay, F-91191 Gif-sur-Yvette Cedex, France*
[16]*STFC Daresbury Laboratory, Daresbury, Warrington, WA4 4AD, United Kingdom*
[17]*Department of Physics and Astronomy, Uppsala University, SE-75120 Uppsala, Sweden*
[18]*Université de Lyon, F-69622, Lyon, France and Université Lyon 1, Villeurbanne; CNRS/IN2P3, UMR5822, IPNL, France*

(Received 3 April 2014; published 2 July 2014)

The properties of pygmy dipole states in ^{208}Pb were investigated using the ^{208}Pb(^{17}O, ^{17}O'γ) reaction at 340 MeV and measuring the γ decay with high resolution with the AGATA demonstrator array. Cross sections and angular distributions of the emitted γ rays and of the scattered particles were measured. The results are compared with (γ, γ') and (p, p') data. The data analysis with the distorted wave Born approximation approach gives a good description of the elastic scattering and of the inelastic excitation of the 2^+ and 3^- states. For the dipole transitions a form factor obtained by folding a microscopically calculated transition density was used for the first time. This has allowed us to extract the isoscalar component of the 1^- excited states from 4 to 8 MeV.

DOI: 10.1103/PhysRevLett.113.012501 PACS numbers: 24.30.Cz, 24.10.Eq, 25.55.Ci, 27.80.+w

A common feature of the strongly interacting many-body quantum systems is the presence of collective phenomena. In nuclei giant resonances (GRs), as the very extensively studied giant dipole resonance (GDR), are well established collective states, with an energy larger than the particle separation energy. For neutron rich nuclei the GDR is characterized by concentrations of strength, denoted as pygmy states, around and below the particle separation energy. Pygmy states are presently attracting particular attention because they reflect a property of neutron rich matter forming neutron skin (see, e.g., [1–7]) with implications to two relevant astrophysics problems, that of neutron stars and of *r*-process nucleosynthesis [8]. The progress in the prediction of the properties of neutron rich matter and of its equation of state is connected to advances in energy density functionals (EDF), an approach also widely used in condensed matter. Theoretical nuclear models based on EDF describe the pygmy states either as a mixing between an isoscalar compressional dipole mode and the GDR (namely, the proton-neutron oscillation

mode), or even as due to the remaining particle-hole strength. Indications of the mixing between the isoscalar compressional mode due to the oscillation of the neutron skin and the p-n oscillation mode have been obtained using (α, α') scattering [9]. While in the first experiments using $(\alpha, \alpha'\gamma)$ the gamma decay of the pygmy dipole resonance (PDR) was measured with low resolution [10], more recently, high resolution measurements were performed for a few nuclei [11–13] including ^{124}Sn and ^{140}Ce (magic in Z and N, respectively). The latter measurements, when compared with results for 1^- states from (γ, γ'), showed that the pygmy strength splits into two parts within the excitation energy 4–9 MeV with different nature. The understanding of the nature of the pygmy resonance is also particularly important in connection with the nuclear polarizability (measured recently in ^{208}Pb [4] and ^{68}Ni [14]), affected by the pygmy states, which gives constraints to the neutron skin and thus to the nuclear equation of state of neutron rich matter.

One important open problem for pygmy states is the cross section sensitivity to transition densities containing the nuclear structure information. To explore this one needs high resolution measurements and comparison of data obtained with different probes. In particular, nuclei with sizable neutron skin, such as the doubly magic ^{208}Pb, are very interesting. In addition, to pin down the effect related to the transition density of the pygmy states, which is peaked on the surface (and thus in the region of the neutron skin), one needs to use probes sensitive to the nuclear surface. This is done for the first time with the new high resolution experiment using the ^{208}Pb(^{17}O, ^{17}O'γ)^{208}Pb reaction at 20 MeV/u reported in the present Letter. In addition, high lying 2^+ states identified in (γ, γ') were seen for the first time with an hadronic probe. Measurements of this reaction with lower resolution for γ rays were previously made at 22 MeV/u [15] [for the giant quadrupole resonance (GQR)] and 84 MeV/u for the GDR [16]. Only the latter showed a strong Coulomb excitation of GDR and since we want a small Coulomb contribution for 1^- states, 20 MeV/u was chosen as the bombarding energy.

The experiment was performed at the tandem-ALPI accelerator complex of the LNL-INFN laboratory, using a 340 MeV ^{17}O beam and a self-supporting ^{208}Pb target 2.8 mg/cm^2 thick. The scattered ^{17}O ions were detected with two segmented $\Delta E - E$ silicon telescopes (pixel type), prototypes for the TRACE project [17,18], placed symmetrically to the beam axis. These telescopes covered the angular range of 12°–25°, allowed a good separation of the oxygen isotopes, and their total energy resolution for the summed signals was approximately 0.3%. The γ rays originating from decays following inelastic excitation were measured with the highly segmented HPGe detectors of the AGATA demonstrator system [18,19]. The ^{17}O beam was chosen, instead of the more abundant ^{16}O, because this nucleus is loosely bound (the neutron separation energy being 4.1 MeV), and thus with the identification of ^{17}O one is basically free from projectile γ rays in the energy region of interest, namely, 4–8 MeV.

The left panel of Fig. 1 shows the γ-ray energy spectrum measured with the AGATA demonstrator and obtained applying a diagonal cut $E_x = E_\gamma$ in the matrix E_x versus E_γ (the width of the cut was 1.5 MeV). The quantity E_x is the excitation energy of the target nucleus deduced from the measured ^{17}O kinetic energy. This γ-ray spectrum was unfolded according to the technique reported in Ref. [20], using the detector response function [21,22] and this resulted in the suppression of the first and second escape peaks and of most of the Compton contribution to the spectrum. The treatment of high-energy γ rays was performed according to [21], and the Doppler correction for the ^{208}Pb recoil velocity resulted in a resolution of 12 keV at 5.5 MeV. The inset in the left panel of Fig. 1 shows the details of the γ-ray spectrum at higher energy. The γ rays identified in this spectrum correspond to well-known $E1$ and $E2$ transitions [23]. By exploiting the high segmentation of the used germanium and silicon detectors one can measure the angular distribution of the emitted γ rays relative to the recoil in an almost continuous fashion. For each event the angle $\theta_{\gamma,\,\mathrm{recoil}}$ between the γ-ray emission and the ^{208}Pb recoil velocity vector was reconstructed. On the right-hand side of Fig. 1 two measured angular distributions, one for the $E1$ transition of 5.512 MeV (top) and the other for the $E2$ transition of 6.194 MeV are shown (bottom). The data in both cases follow remarkably well the expected yield distribution. Note that the excitation with an isoscalar probe of the 6.194 MeV state and two other high energy $E2$ states were measured with their γ decay for the first time in this experiment (see also discussion below).

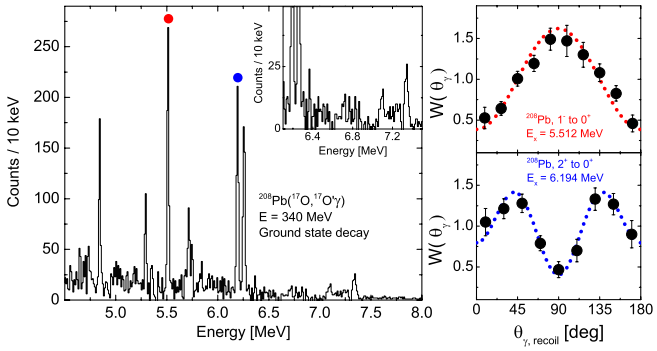

FIG. 1 (color online). Left panel: γ-ray energy spectrum, measured with the AGATA array, corresponding to the ^{17}O scattering channel and with the additional condition for selecting transitions to the ground state. The inset shows the details of the spectrum at high energy. Right panel: the angular distributions of the $E1$ γ-ray transition from the 1^- state at 5.512 MeV (top) and of the $E2$ transition from the 2^+ state at 6.194 MeV. The red (blue) circle and line are for the $E1$ ($E2$) transition at 5.512 (6.194) MeV.

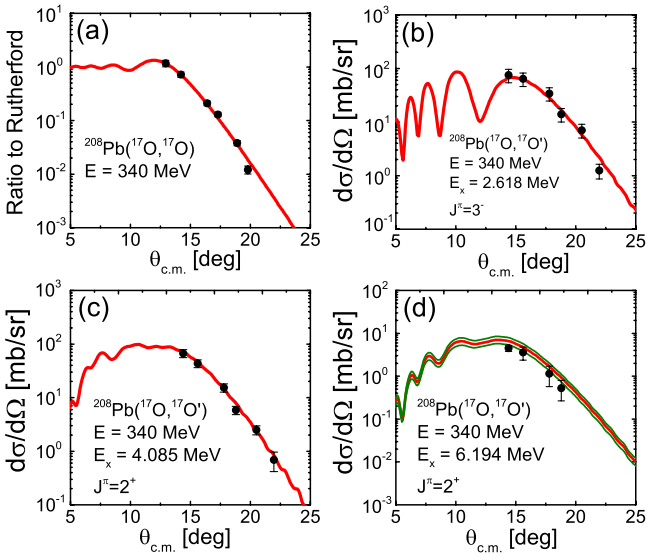

FIG. 2 (color online). Cross section measurements (closed circles) and DWBA predictions (solid curves) for the ^{208}Pb(^{17}O,^{17}O)^{208} and ^{208}Pb(^{17}O,^{17}O$'\gamma$)^{208}Pb at $E_{\mathrm{beam}} = 340$ MeV in the center of mass frame. (a) Elastic-scattering cross section divided by the Rutherford cross section. (b),(c),(d) Cross sections for excited states at 2.618 MeV (3^- state), at 4.085 MeV (2^+ state), and at 6.194 MeV (2^+ state), respectively. The error bars represent the statistical error. The green curves in panel (d) take into account the experimental error in the $B(E2)\uparrow$ value known from (γ, γ') [23,27].

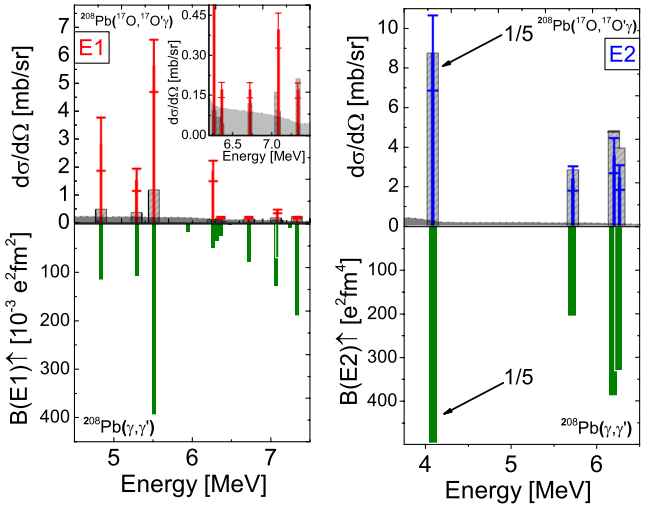

FIG. 3 (color online). Top panels: the measured differential cross section at the average angle of 15.6° for $E1$ transitions (red bars in the left panel) and $E2$ transitions (blue bars in the right panel). The inset shows the details in the higher energy region. The dashed bars give calculated DWBA excitation cross sections using the $B(E1)\uparrow$ and $B(E2)\uparrow$ values from (γ, γ') [23,27] and standard form factors (see text). The shaded areas show the sensitivity limit of the experiment. Bottom panels: electromagnetic reduced transition strength measured with (γ, γ') experiments [23]. The statistical error of the experiment implies lower and upper values indicated with the short horizontal bars.

In Fig. 2 [panel (a)] the data for elastic scattering divided by the Rutherford cross section are shown. The normalization of the calculation to the data at 11.9° gave an overall factor related to the beam current and target thickness. The corresponding distorted wave Born approximation (DWBA) predictions were obtained with the computer code FRESCO [24]. The optical model parameters of Saxon-Woods potentials providing the best fit to the data correspond to $V = 40.0$ MeV, $W = 42.5$ MeV (with V and W the depth of the real and imaginary potentials), $r_v = r_W = 1.15$ fm, $a_V = a_W = 0.767$ fm (the radii and diffuseness of the real and imaginary parts) and $r_C = 1.20$ fm (the Coulomb radius parameter). They are in general good agreement with a previous measurement at a similar energy [15,25].

The optical model parameters from the elastic scattering were then used to calculate the excited states' cross sections. The predictions for the 3^- state at 2.618 MeV and for the 2^+ state at 4.085 MeV used the known $B(E2)\uparrow$and $B(E3)\uparrow$ values [23,26,27] (see Fig. 2). Pure isoscalar excitation was assumed, implying that the ratio of the neutron matrix element M_n and the proton matrix element M_p is given by $M_n/M_p = N/Z$. It is clear from the good agreement with the data on an absolute scale (no further normalization) that the deformed potential does an excellent job. The results for 2^+ and 3^- states are consistent with a measurement at 375 MeV [25]. For the 3^- state a hindrance factor was needed when it was excited with a beam energy of 84 MeV/u [28]. Also, the high-lying $E2$ state at 6.194 MeV is rather well reproduced by the calculation with the condition $M_n/M_p = N/Z$. In general, this implies a dominant isoscalar character of the state, although the work in [15] discussed the validity of this relation in the case of the GQR. All measured cross sections averaged over angles [the average center of mass (c.m.) angle being 15.6°] are shown in the top panels of Fig. 3, with the $E1$ transitions on the left and the $E2$ transitions on the right. The shaded areas in this figure show the sensitivity limit, deduced on the base of the background present in the spectra. In the bottom part of Fig. 3 the $B(E1)\uparrow$ and $B(E2)\uparrow$ values deduced from (γ, γ') measurements [23] are shown. Note that (p, p') data of [4] provide, in the region of interest here, results basically identical to those of (γ, γ').

In the top left panel of Fig. 3 the DWBA predictions for the $E1$ transitions, corresponding to the experimental values of the $B(E1)\uparrow$ from (γ, γ') [23,27] and (p, p') [4], are shown with dashed bars. These calculations, which are in strong disagreement with the data, were obtained using a standard form factor (not pure Coulomb) and are found to be very similar to the Coulomb excitation alone. Examining Fig. 3 one notes a rather strong reduction of the cross section, appearing at first glance anomalous, for the $E1$ states at 6.5–7.5 MeV as compared with those at 4.5–6.5 MeV. This seems to be in contrast with the known

$B(E1)\uparrow$ values and with the fact that the decrease of the number of virtual photons in such a small excitation energy interval is not expected to account for it. On the other hand, the finding that the Coulomb excitation cross section for the 4.5-6.5 MeV transitions is much smaller than the data (it accounts for only 20%—30% of the measured values) indicates clearly that these $E1$ states are excited strongly also by nuclear interaction. This nuclear contribution appears to be different for these two energy intervals and, consequently, this suggests that the nature of the states is not the same.

Another interesting feature of the present experiment is the fact that for the two known closely lying 1^- states at 7.063 and 7.083 MeV, the (^{17}O,^{17}O′) reaction populates only the second state and not the first, in contrast with the fact that the $B(E1)\uparrow$ of the first state is much larger than that of the second. Similarly to what is found for ^{48}Ca [29], this could suggest that these states originate from an isospin pure level which is then split by isospin mixing.

The DWBA predictions for the $E2$ transitions at 4–6.5 MeV are shown with dashed bars in the right panel of Fig. 3. For these calculations the known $B(E2)\uparrow$ values [23] were used. In addition, in all cases the assumption was made that the relation $M_n/M_p = N/Z$ is fulfilled for the proton and neutron matrix elements. For all measured $E2$ transitions the DWBA predictions reproduce rather well the experimental results, in contrast with the $E1$ case.

To understand the measured $E1$ cross sections, we have performed DWBA calculations with a different type of nuclear form factor and using $B(E1)\uparrow$ values known from (γ, γ') [23,27]. In particular, for the most intense $E1$ states at 4.842 and 5.512 MeV the angular distribution of the scattered particles was measured. As discussed above for Fig. 3, one finds that indeed DWBA calculations, with a standard phenomenological nuclear form factor [based on the tail of the GDR and shown with a green dotted curve in panel (c) of Fig. 4], do not account for the data over the entire measured angular range. This is shown in the two top panels of Fig. 4. These calculations (blue dashed lines) do not differ substantially from those including the Coulomb contribution only (green dotted line).

A better form factor is needed for the DWBA calculations. In Ref. [30], a microscopic form factor was calculated for $^{17}\mathrm{O} + {}^{208}\mathrm{Pb}$, by using a double folding procedure with an M3Y nucleon-nucleon interaction. This is shown in panel (c) of Fig. 4 with all the different contributions [Coulomb (dotted-dashed line), nuclear for $L = 1$ and $T = 1$ (dashed line), nuclear isoscalar (long-dashed line)] and together with the standard nuclear potential (green dotted line). The microscopic transition density, shown in the inset, was obtained with a HF + RPA calculation and putting together various 1^- states (at around 7 MeV) with significant strength [2.3% of the isoscalar energy weighted sum rule (ISEWSR)] as in Ref. [30]. The obtained transition density shows the strong isoscalar characteristics of the pygmy

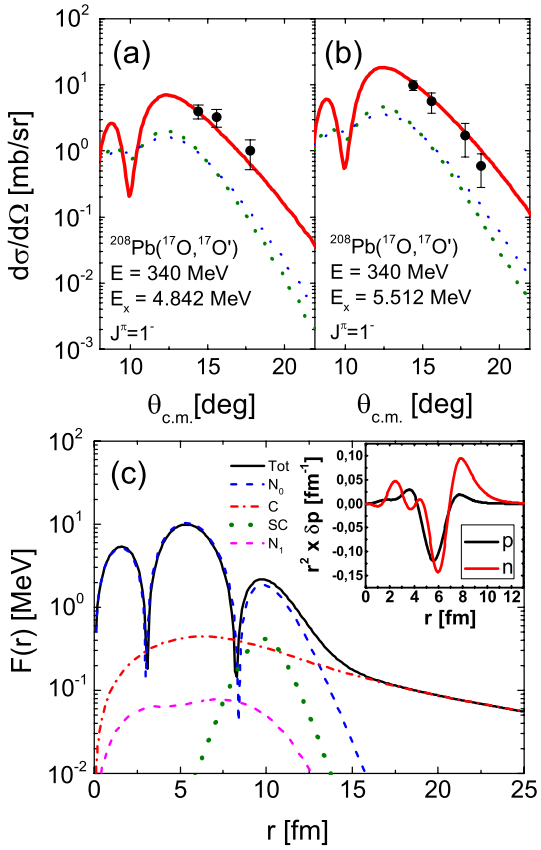

FIG. 4 (color online). Panels (a) and (b) show the inelastic scattering cross section ^{208}Pb(^{17}O, ^{17}O′)208Pb* at 340 MeV for the $E1$ states 4.842 and 5.512 MeV, respectively. The error bars are the statistical errors. The lines show DWBA calculations. The green dotted curves are the Coulomb excitation cross sections and the blue dashed lines are calculations with the standard phenomenological form factor (tail of the GDR). The solid lines include the nuclear contribution calculated with the microscopic form factor shown in the bottom panel [panel (c), see text] and derived with the transition density shown in the inset.

dipole state: neutron and proton transition densities are in phase in the interior and a strong surface contribution due only to neutrons. We note that, in the region physically more significant (between 10 and 14 fm), the most important contribution for the form factor comes from the nuclear part. The DWBA calculations with this form factor and using, respectively, 2.6%, and 3.5% of the EWSR for the isoscalar $E1$ excitation reproduce the data remarkably well. In contrast, the data are not reproduced by calculations without the surface part of the form factor. The values of the ISEWSR were deduced by taking the cross section as a sum of two parts: one being the Coulomb and the other the nuclear (isoscalar in this case) contribution. For the nuclear contribution, the used microscopic form factor corresponded to a 2.3% ISEWSR, value that was used as a starting point to fit the data. In the fit, the Coulomb contribution was fixed and corresponding to the known $B(E1)$ values. The normalization factors (0.4–1.5

including the energy variation among the different states) were then multiplied with the starting value of the ISEWSR, being the isoscalar cross section proportional to it. The extracted values of the ISEWSR for the most intense measured 1^- transitions are 2.6(0.8)% (4.842 MeV), 3.5 (0.5)% (5.512 MeV), 0.92(0.23)% (5.292 MeV), and 1.69 (0.28)% (6.264 MeV). The obtained summed value, including the contribution of all the observed 1^- transitions up to 7.335 MeV, is 9.0(1.5)%, in line with the value reported in [10] and consistent with the fact that most of the isoscalar strength in ^{208}Pb is around 22 MeV [31–33]. It should be also pointed out that the fraction of ISEWSR for the 4.842 MeV $E1$ state was not obtained in the past with $(\alpha, \alpha'\gamma)$ but only from an analysis reported in [10] of a low resolution measurement of (p, p') scattering.

In conclusion, this Letter has presented new data concerning the nature of the pygmy states. The $E1$ transitions cross sections for ^{208}Pb were analyzed for the first time using a microscopic form factor and the isoscalar potential was found to depend on the presence of the neutron skin. A consistent description was obtained for elastic and inelastic excitations of $E2$ and $E3$ states. In addition, three high-lying $E2$ states were excited for the first time with a hadron probe offering the possibility to study proton and neutron multipole matrix elements. The $(^{17}O, ^{17}O'\gamma)$ reaction at around 20 MeV/u is found to be a good tool for these studies so that the loosely bound ^{13}C could be used as a target with intense radioactive beams in inverse kinematics.

The authors wish to thank D. C. Radford for adapting the unfolding program. We acknowledge support from several grants. Contributions from European FP7/2007-2013 under Grant Agreement No. 262010ENSAR; INFN from Italy; from Poland Grants No. DPN/N190/AGATA/2009 and No. 2011/03/B/ST2/01894, No. 2013/09/N/ST2/04093, and No. 2013/08/M/ST2/00591; from Spain Grant No. PROMETEO/2010/101, MINECO Grants No. AIC-D-2011-0746, No. FPA2011-29854, and No. FPA-2011-29854-C04-01.

*angela.bracco@mi.infn.it
†Present address: Department of Physics, University of Oslo, N-0316 Oslo, Norway.
‡Present address: RIKEN Nishina Center, 2-1 Hirosawa, Wako, 351-0198 Saitama, Japan.

[1] A. Klimkiewicz *et al.*, Phys. Rev. C **76**, 051603 (2007).
[2] A. Carbone, G. Colò, A. Bracco, L.-G. Cao, P. F. Bortignon, F. Camera, and O. Wieland, Phys. Rev. C **81**, 041301(R) (2010).
[3] O. Wieland *et al.*, Phys. Rev. Lett. **102**, 092502 (2009).
[4] A. Tamii *et al.*, Phys. Rev. Lett. **107**, 062502 (2011).
[5] X. Roca-Maza, G. Pozzi, M. Brenna, K. Mizuyama, and G. Colo, Phys. Rev. C **85**, 024601 (2012).
[6] X. Viñas, M. Centelles, X. Roca-Maza, and M. Warda, Eur. Phys. J. A **50**, 27 (2014).
[7] N. Paar, D. Vretenar, E. Khan, and G. Colò, Rep. Prog. Phys. **70**, 691 (2007).
[8] S. Goriely, E. Khan, and M. Samyn, Nucl. Phys. **A739**, 331 (2004).
[9] D. Savran, T. Aumann, and A. Zilges, Prog. Part. Nucl. Phys. **70**, 210 (2013).
[10] T. D. Poelhekken, S. K. B. Hesmondhalgh, H. J. Hofmann, A. van der Woude, and M. N. Harakeh, Phys. Lett. B **278**, 423 (1992).
[11] D. Savran, M. Babilon, A. van den Berg, M. Harakeh, J. Hasper, A. Matic, H. Wörtche, and A. Zilges, Phys. Rev. Lett. **97**, 172502 (2006).
[12] J. Endres *et al.*, Phys. Rev. Lett. **105**, 212503 (2010).
[13] J. Endres *et al.*, Phys. Rev. C **85**, 064331 (2012).
[14] D. M. Rossi *et al.*, Phys. Rev. Lett. **111**, 242503 (2013).
[15] J. R. Beene, F. Bertrand, M. Halbert, R. Auble, D. Hensley, D. Horen, R. Robinson, R. Sayer, and T. Sjoreen., Phys. Rev. C **39**, 1307 (1989).
[16] J. R. Beene *et al.*, Phys. Rev. C **41**, 920 (1990).
[17] D. Mengoni, Ph.D. thesis, University of Camerino, 2007.
[18] A. Gadea *et al.*, Nucl. Instrum. Methods Phys. Res., Sect. A **654**, 88 (2011).
[19] S. Akkoyun *et al.*, Nucl. Instrum. Methods Phys. Res., Sect. A **668**, 26, (2012).
[20] D. C. Radford, I. Ahmad, R. Holzmann, R. V. F. Janssens, and T. L. Khoo, Nucl. Instrum. Methods Phys. Res., Sect. A **258**, 111 (1987).
[21] F. C. L. Crespi *et al.*, Nucl. Instrum. Methods Phys. Res., Sect. A **705**, 47 (2013).
[22] E. Farnea, F. Recchia, D. Bazzacco, Th. Kröll, Zs. Podolyák, B. Quintana, and A. Gadea, Nucl. Instrum. Methods Phys. Res., Sect. A **621**, 331 (2010).
[23] T. Shizuma, T. Hayakawa, H. Ohgaki, H. Toyokawa, T. Komatsubara, N. Kikuzawa, A. Tamii, and H. Nakada, Phys. Rev. C **78**, 061303 (2008).
[24] I. J. Thompson, Comput. Phys. Rep. **7**, 167 (1988).
[25] D. J. Horen *et al.*, Phys. Rev. C **44**, 128 (1991).
[26] R. H. Spear, W. J. Vermeer, M. T. Esat, J. A. Kuehner, A. M. Baxter, and S. Hinds, Phys. Lett. **128B**, 29 (1983).
[27] N. Ryezayeva, T. Hartmann, Y. Kalmykov, H. Lenske, P. von Neumann-Cosel, V. Ponomarev, A. Richter, A. Shevchenko, S. Volz, and J. Wambach, Phys. Rev. Lett. **89**, 27 (2002).
[28] J. R. Beene, D. J. Horen, and G. R. Satchler, Phys. Lett. B **344**, 67 (1995).
[29] V. Derya, *et al.*, Phys. Lett. B **730**, 288 (2014).
[30] E. Lanza, A. Vitturi, M. V. Andres, F. Catara, and D. Gambacurta, Phys. Rev. C **84**, 064602 (2011).
[31] B. F. Davis *et al.*, Phys. Rev. Lett. **79**, 609 (1997).
[32] M. Uchida *et al.*, Phys. Lett. B **557**, 12 (2003).
[33] D. H. Youngblood, Y.-W. Lui, H. L. Clark, B. John, Y. Tokimoto, and X. Chen, Phys. Rev. C **69**, 034315 (2004).